A Curve Approximated Hysteresis Model for Steel Bridge Columns

Ji Dang[1], Huihui Yuan[2], Akira Igarashi[3], Tetsuhiko Aoki[4]

Abstract: In this paper, a curve approximated hysteresis model for SDF analysis is proposed to predict the nonlinear response of bridges supported by steel columns with suitable scope of severe damaged deterioration domain. Instead of multiple straight lines, a series of curves are adopted to precisely describe complicated force-displacement hysteresis behavior of the column. The P-δ effect, hardening effect in unloading-reloading hysteresis loops, deterioration of strength and stiffness are taken into account. Parameters of proposed hysteresis model for three types of steel pier specimens used in this study are calibrated by six static cyclic tests. To verify the accuracy of the proposed model, eleven pseudo-dynamic tests are conducted. By comparing the simulation and the test results, the differences between the predicted nonlinear seismic response using the proposed model and pseudo-dynamic tests are found to be, averagely, 5% in maximum response displacement, 22% in residual displacement and 4% in the amount of energy dissipation.

CE Database subject headings: Steel columns; hysteresis; numerical models; pseudodynamic method

1. INTRODUCTION

Collapse of highway bridges during 1995 Kobe earthquake caused loss of function of transportation and delay of emergency support, resulting not only hindrance of post-earthquake restoration process in highly populated Kobe area, but also a tremendous economical impact to Japan. It is evident that ensuring the seismic performance of viaduct bridge piers under strong ground motions is one of the most important issues in maintaining the function of the highway

[1] Program Specific Researcher, Graduate School of Engineering Department of Civil and Earth Resources Engineering, Kyoto University, Kyoto 614-8426, Japan. E-mail: dangji1980@yahoo.co.jp

[2] Doctor course student, Department of Civil Engineering, Aichi Institute of Technology, Toyota, Aichi 470-0356, Japan. E-mail: macarians@gmail.com

[3] Associate Professor, Graduate School of Engineering Department of Civil and Earth Resources Engineering, Kyoto University, Kyoto 614-8426, Japan. E-mail: igarashi.akira.7m@kyoto-u.ac.jp

[4] Professor, Department of Civil Engineering, Aichi Institute of Technology, Toyota, Aichi 470-0356, Japan. E-mail: aoki@aitech.ac.jp

transportation system after strong earthquakes.

To date, a number of monotonic and quasi-static loading tests [1]-[5] have been conducted to investigate the seismic performance of steel bridge piers. Experimental studies by means of pseudo-dynamic tests [6]-[8] revealed that the seismic performance of the steel bridge piers is sensitively influenced by their nonlinear hysteresis behavior. To predict the nonlinear seismic response of steel piers involving the hardening and deterioration behavior, Suzuki et al. proposed a tri-linear type hysteresis model (the two-parameter model) [9] expressed by a combination of lines with three tangential slopes representing the elastic stiffness, hardening stiffness and deterioration stiffness designated by several hysteresis rules. In this model, since the hardening stiffness is decided by the peak load points which will be changed due to deterioration loading history, the overall shape of the hysteresis loop is sensitively influenced by the accuracy of the peak load points' prediction hysteresis rules. However, precise prediction of the peak load points due to deterioration is generally difficult even when the experienced maximum displacement and energy absorption have been taken into account.

Kindaichi et al. proposed a hysteresis restoring force model using the concept of damage index [10], in which the problem of the two-parameter tri-linear type hysteresis model is circumvented by eliminating the need of any prediction for the displacement change of peak load due to deterioration. The damage index indicates the degree of damage in a steel column during the ground shaping, and is used to measure the of strength and stiffness deterioration due to both the maximum experienced displacement and cyclic loading energy dissipation.

In contrast to those conventional hysteresis models using the piecewise linear functions, the horizontal force-displacement relationships are generally observed to consist of smooth curves from the loading test results. This observation motivates to create more proper hysteresis model by improved curve fit approximation of hysteresis loops [11]. In fact, the FEM analysis using stress-strain constitutive relationships defined by continuous curves provides better accuracy than that of analysis using bi-linear or tri-linear stress-strain relationships [12].This motivation is also being encouraged by the need of taking the uncertainty of earthquake level into account in seismic design [13], where the fast, precise and severe deterioration damage analysis suitable numerical method is essential [14].

In this study, a hysteresis model using a series of smooth curves to express the hysteresis restoring force-displacement relationship is proposed to simulate the nonlinear hysteresis response of the steel bridge piers. The hardening effect due to unloading-reloading is considered, and the concept of cumulative deterioration displacement is introduced to evaluate the damage of steel piers caused by local buckling. Moreover, the distance between two peak points due to the cumulative deterioration displacement is studied and it is found that the new displacement of peak load points can be predicted precisely by the peak load points' distance to cumulative deterioration displacement relationship.

Finally, to discuss the accuracy of the proposed hysteresis model, a series of quasi-static tests and

pseudo-dynamic tests are conducted using stiffened square-section steel bridge pier specimens and 6 uni-directional strong ground motion accelerograms designated by highway bridge seismic design specification of Japan [15]. By comparing the test results and dynamic response obtained by numerical analysis, validity of using the proposed model in nonlinear single degree of freedom time history analysis is verified.

2. CURVE APPROXIMATED HYSTERESIS MODEL FOR STEEL BRIDGE PIRES

2.1 Equivalent horizontal force H_{eq}

To consider the $P-\delta$ effect of columns under vertical axial force and horizontal loading, the relationship between the horizontal force H and displacement δ is replaced with the relationship between the equivalent horizontal force H_{eq} and displacement δ. As shown in Fig.1, the base section bending moment M_B, induced by the horizontal force H and the axial force P, can be expressed by Eq. (1).

$$M_B = Hh + P\delta \tag{1}$$

Based on this expression, the equivalent horizontal force H_{eq} is defined as the horizontal force acting at the height h that generates the base moment M_B including the $P-\delta$ effect.

$$H_{eq} = M_B/h = H + P\delta/h \tag{2}$$

2.2 Outline of curve approximated hysteresis model

The hysteresis loops in terms of $H_{eq}-\delta$ relationship for steel piers can be approximated by the combination of (A) basic curve, (B) sub curve and (C) deterioration curve, as illustrated in Fig.2. The basic curve, which starts from the initial point at the onset of loading or an unloading point and ends at a peak load point, as shown Fig.2, is used to represent the $H_{eq}-\delta$ curve in the elasto-plastic region before the peak load point.

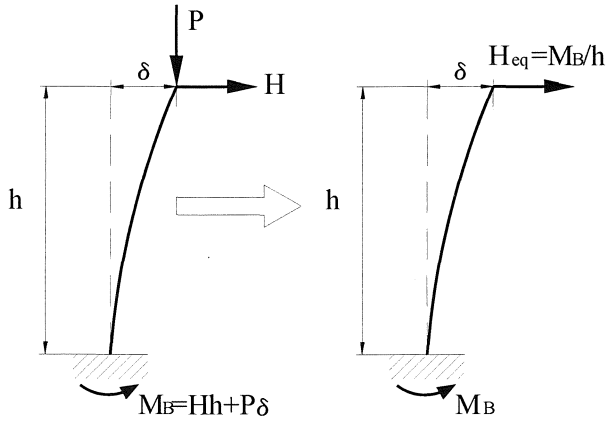

Figure 1. Definition of equivalent horizontal force H_{eq}

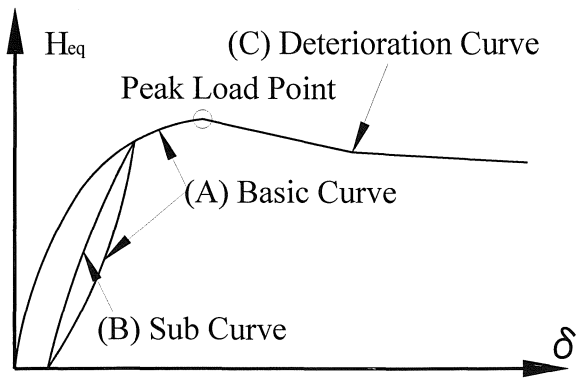

Figure 2. Outline of curve approximated model

The sub curve, which connects two unloading points, is used to approximate the hardening phase of the hysteresis loop when the pier is reloaded back to a former unloading point. Finally, the deterioration curve, which starts from a peak load point, is used to express the horizontal force reduction due to local buckling.

It is also can be seen from the figure that the skeleton curve, the $H_{eq} - \delta$ relationship under monotonic loading, can be expressed by combination of a basic curve (the first half before the peak load point) and a deterioration curve (the second half after the peak load point).

2.3 The basic curve

It is observed in test results that the tangential slope of the horizontal load-displacement hysteresis curve continuously changes from the initial elastic K_e to zero. The degree of this decrease of stiffness is generally severer in neighborhood of the peak point than in the small displacement range and the slope changing tends to be small as the zero point of the hysteresis curve. Assuming that rate of the slope decreasing take place with a constant degrading acceleration, which means the second derivation of $H_{eq} - \delta$ curve is a constant value, accordingly, the basic curve of the $H_{eq} - \delta$ relationship can be expressed by the following cubic polynomial.

$$H_{eq} - H_s = K_e(\delta - \delta_s) + \alpha_1(\delta - \delta_s)^2 + \alpha_2(\delta - \delta_s)^3 \tag{3}$$

In the above equation, δ_s and H_s are the displacement and equivalent horizontal force corresponding to the origin point of the basic curve. For the virgin loading path, as curve 1 in Fig3, the origin point is taken as the point O. For the loading path *i*, the origin point is taken as the point of the unloading from the previous loading path *i*-1. For example, the origin point of the curve path 2 is the unload point A of loading path 1.

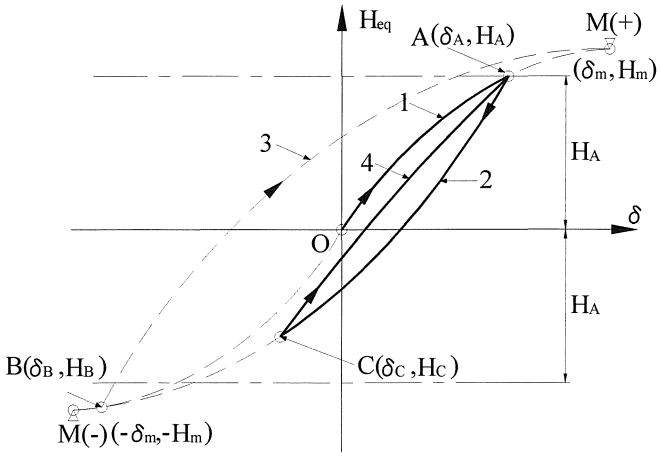

Figure 3. Basic curves and sub curves

The parameter K_e in the above equation denotes the elastic stiffness of the steel pier. It

represents the initial tangential slope of the basic curve at the origin point. The parameters α_1 and α_2 designate how the tangential slope of the basic curve reduces from the elastic stiffness K_e to the tangential slope at the destination point of the basic curve (δ_t,H_t). Further, the constant degrading acceleration is $\alpha_2/6$ and the initial degrading rate is $\alpha_1/2$.

Usami [1] [2] [3], Suzuki [7] and Iura [16] pointed out that the peak load H_m and the corresponding displacement δ_m of the steel pier are solely associated with the geometry and material parameters, and are independent of the loading history. Therefore, the peak load points in positive and negative directions, (δ_m, H_m) and ($-\delta_m$,$-H_m$) in Fig.3, are used as the destination points of the basic curves in each loading directions, respectively. The tangential slope of the basic curves should be zero at peak points, as the loading hysteresis curve reaches its maximum or minimum at these points. Based on these conditions, parameters α_1 and α_2 can be determined by the following expressions.

$$\alpha_1 = 3(H_t - H_s)/(\delta_t - \delta_s)^2 - 2\,K_e/(\delta_t - \delta_s) \tag{4}$$

$$\alpha_2 = K_e/(\delta_t - \delta_s)^2 - 2(H_t - H_s)/(\delta_t - \delta_s)^3 \tag{5}$$

In the above equation δ_t and H_t designate the destination peak load points (δ_m, H_m) or ($-\delta_m$,$-H_m$). For example, the curve 1 in Fig.3 is a positive side basic curve. Its destination point (δ_t, H_t) is the peak load point of positive direction (δ_m, H_m). Similarly, the destination point (δ_t, H_t) for negative direction curve 2 is the peak load point in negative side ($-\delta_m$,$-H_m$).

When loading direction reverses, a new section of hysteresis curve $n+1$ starts form the unloading point ($\delta_{u,n}$, $H_{u,n}$) of the previous curve section n, and the destination point ($\delta_{t,n+1}$, $H_{t,n+1}$) must be specified.

The next curve section can be determined as a basic curve by Eqs. (3), (4) and (5), and its destination point ($\delta_{t,n+1}$, $H_{t,n+1}$) can be specified as the peak load point of reversed direction, only if the following condition is satisfied.

$$|H_{u,n}| > |H_{s,n}| = |H_{u,n-1}| \tag{6}$$

where $H_{s,n}$ is the force of the origin point of the current curve section n, it also equals to the unloading point's force of previous curve if there is a previous curve (n>1). The above condition represents a situation such that the loading amplitude gradually increasing involving a higher plastic deformation level. For example, since unloading from curve 1 at point A(δ_A, H_A) can be shown to satisfy Eq. (6) by substituting $H_{u,n} = H_A$, $H_{s,1} = 0$, and the Eq. (6) becomes $|H_A|$>0. And curve 2 in the Fig. 3 is specified as the next basic curve. It is clear that unloading form a virgin loading path or a skeleton curve will always satisfy Eq.(6) as the curve starts form 0 force.

Another example is the case unloading at point B(δ_B, H_B) from curve path 2. This will lead to another new basic curve 3, as $|H_B| > |H_A|$ which can be seen form the Fig. (3).

2.4 The sub curve

In case such that the condition Eq. (6) is not satisfied as unloading at point C from curve 2 in Fig.3, as the force of point C is smaller than experienced force in point A, $|H_C| > |H_A|$. So that a proper loading path, consistent with common experimental phenomenon, should be the reloading back path to former unloading point. In the case if unloading from point C, loading path should first reload back to point A. After that, loading path will continue through the unfinished part of previous curve 1.

An illustrative example of this case is curve 4. A loading path connecting two unload points, such as curve 4, is approximated by a quadratic represented by Eq. (3) with α_2 =0 and α_1 given by following expression.

$$\alpha_1 = (H_t - H_s)/(\delta_t - \delta_s)^2 - K_e/(\delta_t - \delta_s) \tag{7}$$

in which (δ_t, H_t) and (δ_s, H_s) should be points A and C.

On the other hand, the curve section from unloading in the middle of a sub curve is specified as another renewed sub curve. The all information as origin points and parameters α_1 and α_2 for former basic or sub curve will be restored. These restored curves will be reinstalled in case of reload back from a lower level sub curve reloading path.

The hysteresis rules described above can be summarized by a flowchart shown in Figure 4. By this flow chart, it can be seen that unloading from current basic curve will active the step of judging the type of next curve, basic or sub curve, using Eq.(4). It should be noticed that unloading from the first curve path (the skeleton curve) will directly lead to generate a new basic curve, as the skeleton curve starts from the point of zero force.

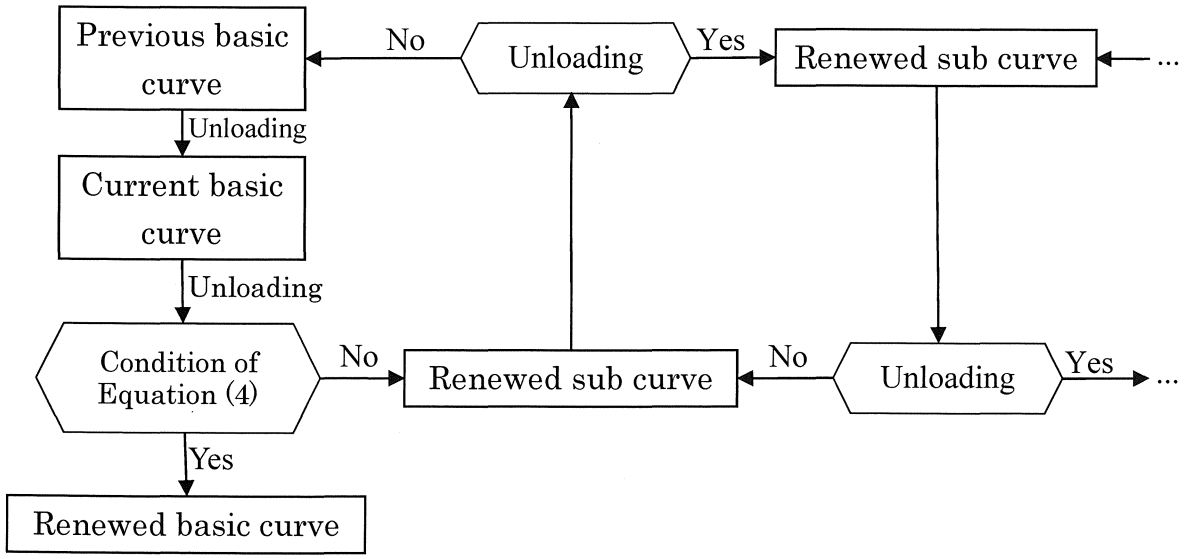

Figure 4. Flow chart of curve selection rules for proposed hysteresis model

Once the renewed basic curve become current basic curve n, the former basic curve n-1 become previous basic curve, and former previous basic curve n-2 will not be used and can be forget. Thus, there are two basic curves should be restored in memory, the current basic curve and the previous basic curve.

If there is no unloading from sub curve, the loading path will go back to continue the previous basic or sub curve. All previous sub curves should be restored to prepare the going back path from deep down low level sub curves as marked as "…" in the figure.

2.5 Cumulative deterioration displacement

Figure 5 shows a schematic representation of a loading hysteresis curve exceeding peak load point M(δ_m, H_m). The deterioration starts from the peak load point M(δ_m, H_m) and ends at the unloading point U(δ_u, H_u). The displacement path experienced in this deterioration section can be expressed as $\delta_d = \delta_u - \delta_m$. Denoting the displacement path length during deterioration experienced in the past i^{th} half cycle as $\delta_d^{(i)}$, and current half cycle is the n^{th} half cycle, the cumulative deterioration displacement (CDD) is calculated by the following equation, while the current displacement δ exceeds δ_m.

$$\text{CDD} = \sum\left|\delta_d^{(i)}\right| + |\delta - \delta_m| \tag{8}$$

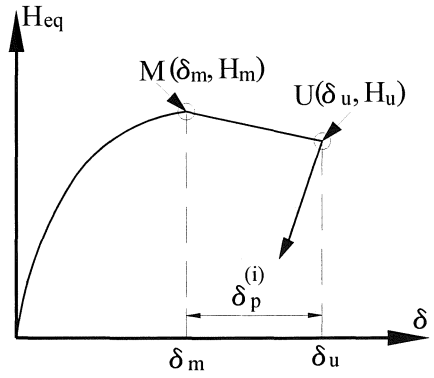

Figure 5. Modeling of Deterioration

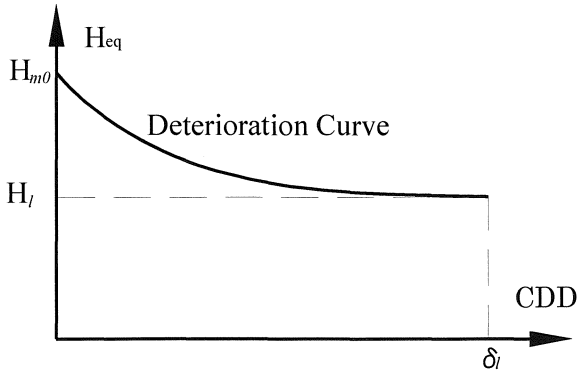

Figure 6. Deterioration Curve

2.6 Deterioration curve

The following quadratic polynomial is used to describe the relationship between the equivalent horizontal force H_{eq} and the cumulative deterioration displacement *CDD*.

$$H_{eq} = H_{m0} + (H_{m0} - H_l)(CDD/\delta_l - 2)CDD/\delta_l \tag{9}$$

where H_{m0} is the initial peak load, δ_l and H_l are the limit displacement and equivalent horizontal force, respectively. The term $(H_{m0} - H_l)$ defines the range of strength deterioration, as

can be seen in Fig.6. By this equation, when *CDD* reaches the limit value δ_l, the equivalent horizontal force H_{eq} converges to H_l, on the same time the slope of deterioration curve will near to 0. This account for the experimental phenomenon acquired in loading tests for thin-walled steel columns. The horizontal force of steel column drops generally fast when local buckling begins, but the deterioration becomes slower and slower due to continues loading. Finally, horizontal force drops suddenly and collapses as losing vertical direction supporting capacity.

2.7 Deterioration of elastic stiffness

The elastic stiffness K_e becomes generally lower than its initial value K_{e0} after experiencing the deterioration. The degree of stiffness degradation is usually associated with the cumulative damage due to local buckling. The deteriorated elastic stiffness K_e corresponding to cumulative deterioration displacement *CDD* is decided by the linear equation as flowing:

$$K_e/K_{e0} = 1 - \kappa CDD/\delta_l \tag{10}$$

where κ is a 0~1 parameter to express the rate of stiffness deterioration of stiffness when the deterioration. The value of κ can be simply set as 0 when the deterioration of elastic stiffness can be omitted as following cases.

a) Analyses for thick-walled steel columns or steel columns properly filled by concrete, which usually do not appear their deterioration behaviors clearly under seismic loading.
b) Analyses for seismic design setting seismic performance limit as δ_{m0} or δ_{95} ($> \delta_{m0}$, the displacement that horizontal force deteriorated until the 95% of H_{m0}). Under this deformation level, the effect of elastic stiffness softening is small enough to be safely omitted.

2.8 Updating of peak load points

The peak points in the positive and negative directions are to be updated as a result of plastic deformation and associated deterioration in either of the loading directions. The rule for update of the peak load points is illustrated in Fig7.

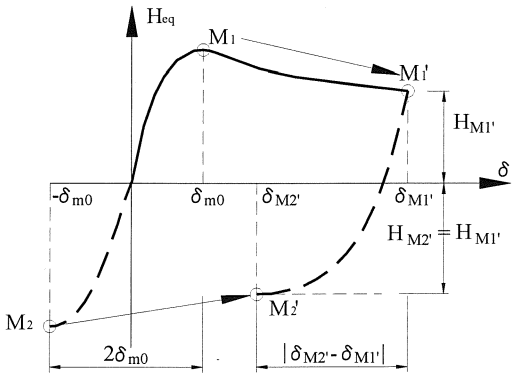

Figure 7. Hysteresis rules after deterioration

In the direction of ongoing plastic deformation, the peak load point M_1 is updated to the new peak point M'_1, which also is the unloading point of the hysteresis curve. The peak point of the opposite direction M_2 is updated to M'_2.

As a simplified assumption, the residual strengths in both directions simultaneously decrease during deterioration. Thus, the load of M'_2 with the opposite sign as expressed by

$$H_{m'2} = -H_{m'1} = H_{eq}(CDD) \tag{11}$$

where $H_{m'1}$ and $H_{m'2}$ are the load values of M'_1 and M'_2, respectively. They share the same absolute value which is decided by the cumulative deterioration displacement *CDD* following the Eq.(9).

The displacement value of the updated peak load point M'_2, denoted by $\delta_{m'2}$ is determined by the specifying a rule for the distance between the two updated peak points $|\delta_{m'2} - \delta_{m'1}|$ as a function of the cumulative damage due to local buckling, where $\delta_{m'1}$ is the displacement value for M'_1. In a manner similar to express the stiffness degradation by Eq. (8), the increase of displacement distance between the two peak load points can be approximately represented by Eq. (10) as a linear function of the cumulative deterioration displacement (*CDD*).

$$|\delta_{m2\prime} - \delta_{m1\prime}|/2\delta_{m0} = 1 + \gamma CDD/\delta_l \tag{12}$$

where δ_{m0} is displacement of the initial peak load point. The reality value of γ is generally between 0 and 1. It can also be set as 0 to omit this effect.

3. PARAMETER IDENTIFICATIONS BY QUASI-STATIC TESTS

The parameters of the hysteresis curve model described in the preceding section required to be provided for conducting the numerical simulation are:

I. Initial peak load point (δ_{m0}, H_{m0})

II. The limit deterioration point (δ_l , H_l)

III. Parameter to express the descending rate of elastic stiffness (κ)

IV. The parameter to express the expansion rate of distance between the two peak points in both directions (γ)

Other contents, such as K_{e0}, can be provided by theoretical evaluation.

In this study, a series of quasi-static loading tests of stiffened the box-section steel bridge piers conducted to identify appropriate values of the parameters I through IV are described.

However, in practice seismic design, calibration of parameters for nonlinear models by loading test is generally difficult, but it can be accomplished by using nonlinear FEM static analysis result

or use empirical equations. To date, more and more engineers and researchers recommend combining the static FEM analysis and SDF nonlinear dynamic simulation [12, 14]. For fast trying of this hysteresis model or simplified seismic design without any complicated FEM analysis, quick setting of the parameters using empirical equations are also introduce here after.

3.1. Test specimens

Three types of test specimens, with the same square-section and different diaphragm stiffener intervals, are used for the quasi-static loading tests. Figure 8 and 9 show the elevated and plan section views of specimens. The specimens with diaphragm intervals of 450mm, 225mm, and 150mm are prepared and referred as D450, D225 and D150, respectively. All specimens of 450mm width square section piers were made with 6 mm thick plates of SM490 steel. The dimensions of specimens are listed in Table 1.

As shown in Fig. 9, two rib stiffeners are attached to each inner surface of the box section. Two specimens for each type are used for the cyclic loading tests. The geometrical parameters of specimens are listed in Table 2. The width-thickness ratio parameters R_R, R_F and the slenderness ratio parameter λ are calculated by the following equations [17].

$$R_R = \frac{b}{t}\sqrt{\frac{\sigma_y}{E}\frac{12(1-v^2)}{\pi^2 k_R}} \quad (13)$$

$$R_F = \frac{b}{t}\sqrt{\frac{\sigma_y}{E}\frac{12(1-v^2)}{\pi^2 k_F}} \quad (14)$$

$$\lambda = \frac{2h}{r}\sqrt{\frac{\sigma_y}{E}} \quad (15)$$

$$k_R = 4n \quad (16)$$

$$k_F = \frac{(1+\alpha^2)^2 + n\gamma_l}{\alpha^2(1+n\delta_l)} \quad (17)$$

Table 1. Geometry sizes of specimens

Specimen	D450	D225	D150
b (mm)	450		
t (mm)	6		
b_S (mm)	55		
D (mm)	450	225	150
t_S (mm)	6		
h (mm)	2400		
A (mm^2)	13300		
I (mm^4)	4.06×10^8		

Table 2. Geometrical parameters of specimens

Specimen	R_R	R_F	λ	λ_s	γ/γ^*
D450	0.517	0.336	0.397	0.368	2.5
D225		0.170		0.183	10.5
D150		0.113		0.123	26.7

where α is the aspect ratio of the plate; α_0 is the limit aspect ratio, γ_l is supplementary member's stiffness ratio; δ_l is the ratio of the area of each supplementary member to the whole section area; b and t are the width and thickness of each steel plate; r is the equivalent radius of the cross section; h is the effective height of the pier model; k_R, k_F are the buckling coefficients given by Eqs.(16) and (17), respectively. λ_s is the slenderness parameter for stiffeners, γ^*s the ratio of optimum

stiffness ratio for supplementary members (stiffeners and diaphragms) [17].

3.2. Loading procedure

Quasi-static loading tests of the specimens are conducted. Displacement is consecutively imposed to the top of specimens in accordance with a specific horizontal displacement pattern under a constant axial vertical load of P=648 kN. The constant axial vertical load P corresponds to 0.15 times the axial yield strength P_y =4320 kN, determined by the nominal yield stress of SM490 and the cross-section area. Firstly, the yield displacement δ_y and yield force H_y were determined in the first cycle ended when strain of steel plate nearing the base cross-section reaches yield strain. The basic displacement pattern is a consecutively increasing cyclic loading path with target displacement amplitudes of $\pm 0.5\delta_y$ (one cycle), $\pm 1\delta_y$ (three cycles),$\pm 1.5\delta_y$(one cycle), $\pm 2\delta_y$ (3 cycles), and so on. After the initial peak load point has been achieved, the displacement path amplitude becomes to 1 δ_y, until the maximum horizontal force for a half cycle loading reduce to the yield force H_y due to deterioration. Exception is the first quasi-static test of specimen D450, in which the displacement path amplitude is increased by 1 δ_y after two loading cycles until reaching the initial peak load point.

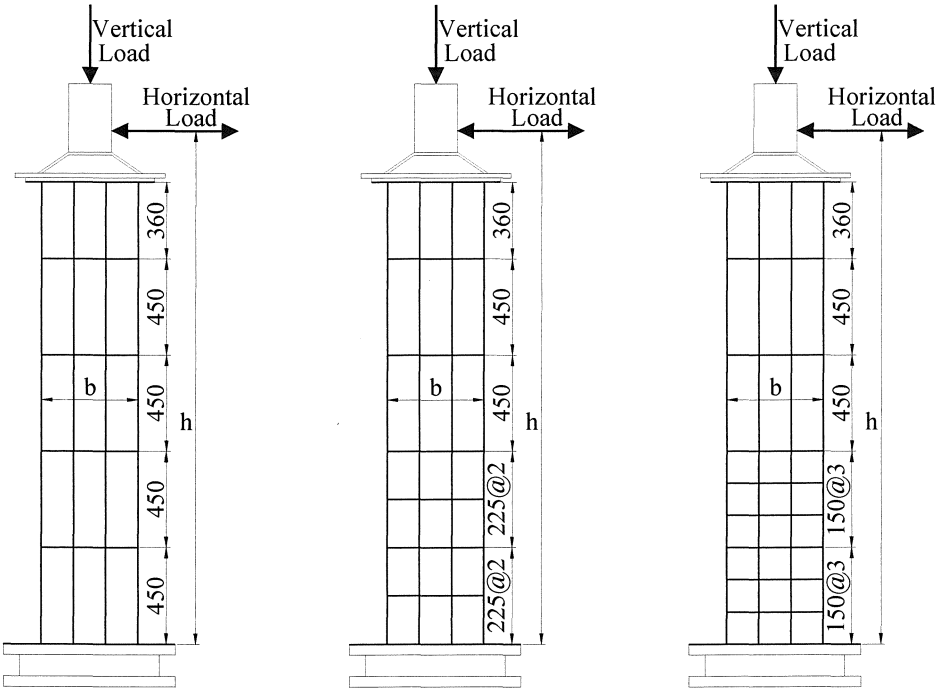

(a) Specimen D450 (b) Specimen D225 (c) Specimen D150

Figure 8. The side views of specimens

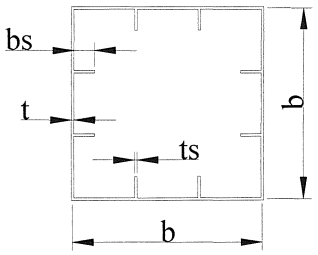

Fig.9 Plan section view

3.3 Test Result

Tensile coupon tests for each pier specimen type were conducted before quasi-static test. The result of tensile coupon tests is shown in Table 3.

Quasi-static loading tests were conducted using two specimens for each pier type, which are called as D450-1, D450-2, D225-1, D225-2, D150-1 and D150-2, respectively. The yield displacement δ_y and yield force H_y are shown in Table 4. The value of δ_y and H_y, and the initial elastic stiffness K_{e0} were determined by averaging the test results of two specimens for each specimen type. Figures 10 (a) ~ (f) indicate the load-displacement relationship obtained by the tests and numerical simulation of proposed method. The horizontal load H and the displacement δ are shown using the none-dimensional axes normalized by H_y and δ_y, respectively.

The initial peak load points (δ_{m0},H_{m0}) obtained as the average values of those from two test results for various specimen types are listed in Table 4.

Table 3. Result of material tests

Specimen	Yield stress σ_y (N/ mm^2)	Yield strain ε_y ($\times 10^{-6}$)	Young modulus E (N/ mm^2)	Maximum stress σ_u (N/ mm^2)
D450	415	1961	2.25×10^5	568
D225	409	2011	1.98×10^5	546
D150	384	1858	2.07×10^5	505

Table 4. Hysteresis parameters from quasi-static tests

Specimen	δ_y (mm)	H_y (kN)	K_{e0} (kN/ mm)	δ_{m0} $/\delta_y$	H_{m0} $/H_y$	δ_l $/\delta_y$	H_l $/H_y$	κ	μ
D450	12.4	201	16.3	3.44	1.71	21.4	1.02	0.51	0.38
D225	15.0	238	15.9	2.57	1.71	13.3	1.11	0.04	0.13
D150	14.8	242	16.4	2.45	1.61	14.9	0.99	0.24	0.10

The cumulative deterioration displacement CDD for each test case was obtained by accounting for the displacement path length of loading history that falls within the range of force deterioration. The relationships between H_{eq} and CDD are shown in Fig.11. The $H_{eq} - CDD$ is approximately expressed by Eq.(9) by the least-square curve fitting. As the direct curve fitting for Eq.(9) may difficult for uniformed LS computer program, following equation can be used as a temporary substitution of Eq.(9).

$$H_{eq} = H_{m0} + \beta_1 CDD + \beta_2 CDD^2 \tag{18}$$

where β_1 and β_2 are the first and second order coefficients of the second-order polynomial function. So that the parameter $\beta_1$and β_2 can be easily obtained by a typical LS program. The approximated deterioration curves are plotted with solid lines in Fig.11. In this case, the limit point (δ_l,H_l) in Eq.(9) can be represented by following expressions.

$$\delta_l = -0.5\beta_1/\beta_2 \tag{19}$$

$$H_l = H_{m0} - 0.25\beta_1{}^2/\beta_2 \tag{20}$$

The calculated value of δ_l and H_l are shown in Table 4. Deterioration of the stiffness K_e and expansion of peak load point distance $|\delta_{m2\prime} - \delta_{m1\prime}|/2\delta_{m0}$ respected to CDD are shown in Figures 12 and 13, respectively. Applying Eqs. (10) and (12) to regress these results, the values of parameters κ and γ can also be obtained by the same regression procedure. All the calibrated values of these parameters are listed in Table 4.

In Fig.10, the H-δ hysteresis curves simulated by the curve approximation model with parameters identified from the quasi-static loading are shown with broken lines. A close agreement between the curves calculated by the model and that of the test results can be observed in the figures.

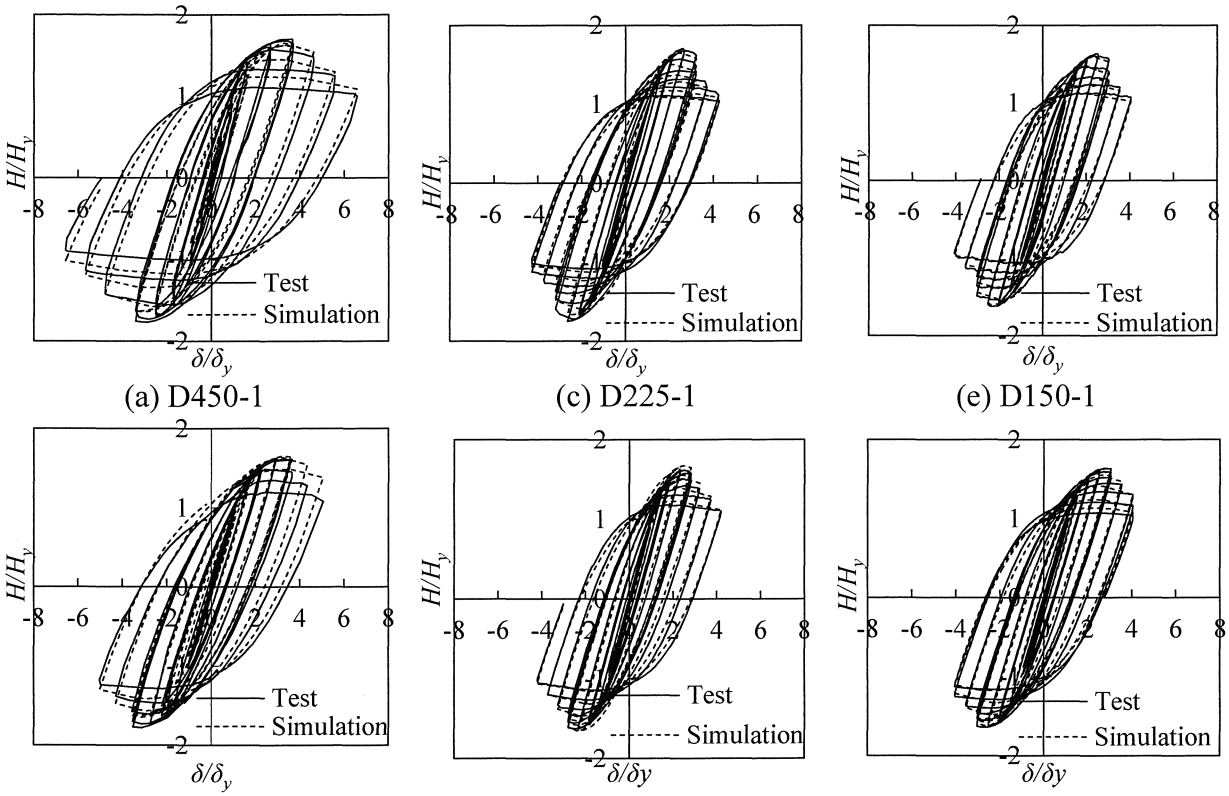

Figure 10. H-δ relationships obtained by cyclic loading tests and numerical simulation

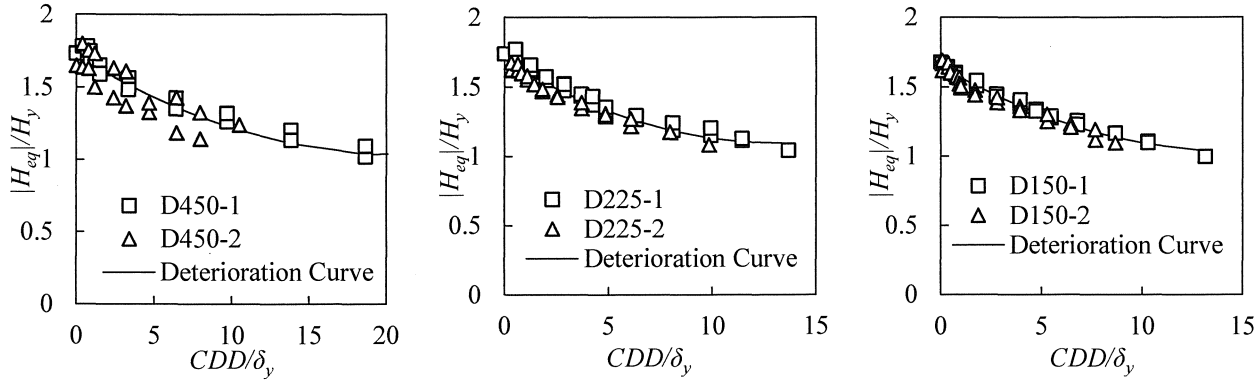

Figure 11. The relationships of H_{eq} and CDD

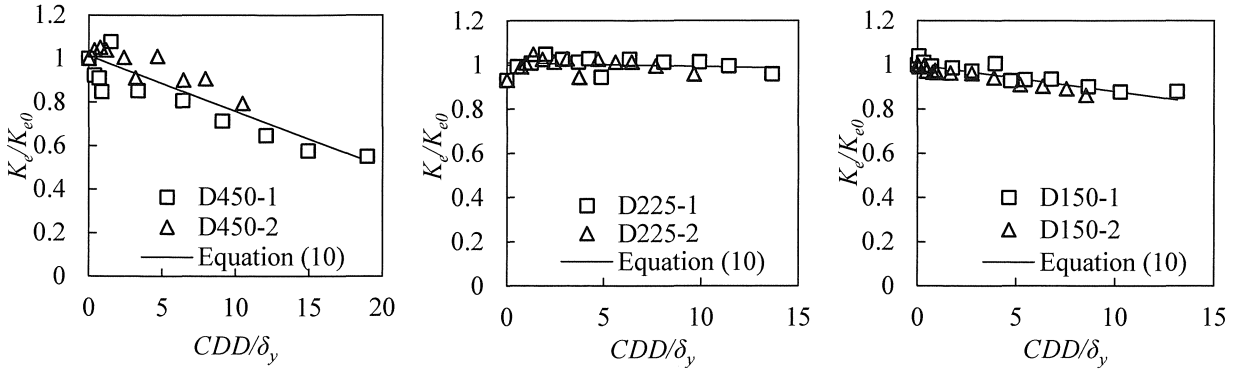

(a) D450 (b) D225 (c) D150

Figure 12. Deterioration of elastic stiffness

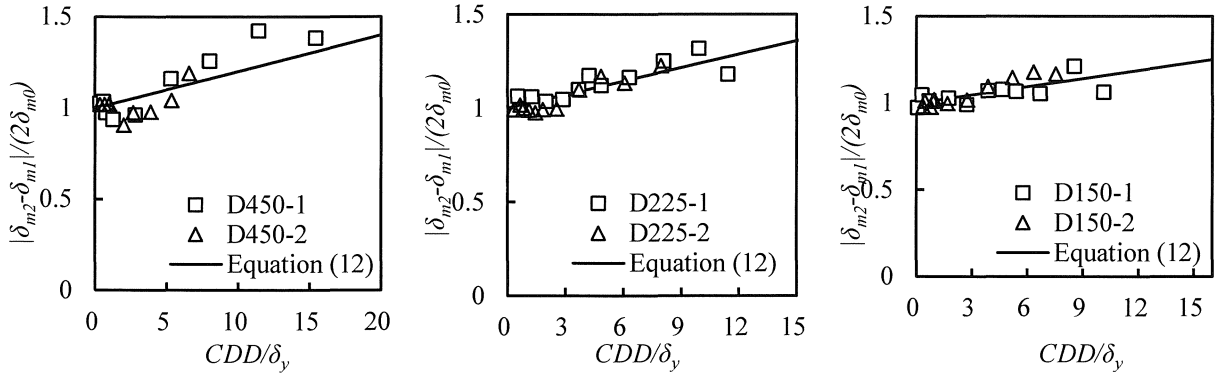

(a) D450 (b) D225 (c) D150

Figure 13. Increase of peak load point distance after deterioration

3.4 Simplified settings of parameters

Effective range of proposed model is from 0 to the limit point displacement δ_l, includes the elastic stage, hardening stage, deterioration stage but not collapse stage. Generally, the peak load will be 1.5~2.0 times of yield force (H_m=1.5~2.0H_0), and its corresponding displacement is from 2.0 ~5.0 times of yield displacement (δ_m=2.0~5.0δ_0). Well-stiffened or thick-walled columns (0.3<R_R<0.5, 0.3<λ<0.5) can acquire larger peak load and better ductile. Ge and Usami etc. gave following empirical equation to evaluate the maximum force and corresponding displacement and the displacement of load deteriorate to 95% of peak load[18].

$$H_m/H_0 = 0.1/\sqrt{R_F\lambda\bar{\lambda}'_s} + 1.06 \quad (21)$$

$$\delta_m/\delta_0 = 0.2/(R_F\sqrt{\lambda}\bar{\lambda}'_s) + 1.2 \quad (22)$$

$$\delta_{95}/\delta_0 = 0.25/((1 + P/P_y)R_F\sqrt{\lambda}\bar{\lambda}'_s) + 2.31 \quad (23)$$

$$\bar{\lambda}'_s = \sqrt{\sigma_y/E}D/(\pi r_s\sqrt{Q}\sqrt[5]{\alpha}) \quad (24)$$

$$Q = \frac{1}{2R_R}(1.33R_F + 0.868 - \sqrt{(1.33R_F + 0.868)^2 - 4R_R} \leq 1 \quad (25)$$

where r_s is the radius of gyration of the T cross-section made of a stiffener and its stiffened panel. Similar equations for κ and γ can be roughly regressed from the test result and the geometry parameter R_F which can be found in Tables 4 and 2, respectively.

$$\kappa = 1.58R_F - 0.06 \qquad 0 \leq \kappa \leq 1 \qquad (26)$$

$$\gamma = 1.31R_F - 0.07 \qquad 0 \leq \gamma \leq 1 \qquad (27)$$

Accordingly, a simplified empirical equation based approach to set the parameters is as following.

I. Initial peak load point (δ_{m0}, H_{m0}) can be acquired by Eqs. (21) and (22).

II. Set H_l =H_0, and δ_l can be derived by substitute point ($\delta_{95} - \delta_{m0}$, $0.95H_{m0}$) into Eq.(9), where δ_{95} is calculated from empirical Eq. (23).

III. Set the descending rate of elastic stiffness κ by Eq.(26).

IV. Set the expansion rate of peak points distance γ by Eq.(27).

Further, sometimes macroscopic estimation of seismic response of structures is necessary, as analysis used in risk evaluation or decision-making analysis. In these cases, rough but simple setting can be used as δ_{m0}=$3\delta_0$, $H_{m0} = 1.5H_0$, δ_l =$20\delta_0$, H_l =H_0, κ=0 and γ=0. But it should be noticed that these values are only empirical settings for proposed model to keep calculation running correctly and somehow represent the essential hysteresis character of common thin-walled non-concrete-filled steel columns.

4. EXPERIMENTAL VERIFICATION

Pseudo-dynamic tests are conducted to validate the accuracy of the proposed model. The specimens D450, D225 and D150 were used as 1/4 and 1/6 scaled bridge piers for the pseudo-dynamic tests. Newmark's β method (β=1/6) is applied as the time integration scheme for the equation of motion to compute the displacement predictor using the initial stiffness [19, 20]. A time interval of Δt=0.01 sec and a damping ratio of h = 0.05 were used. The following six accelerograms of the 1995 Kobe Earthquake [15] were used as the input ground acceleration:

1,2. NS and EW components recorded at Japan Meteorological Agency (JMA-NS, JMA-EW, Ground Type I);

3,4. NS and EW components recorded at JR Takatori station (JRT-NS, JRT-EW, Ground Type II);

5,6. NS and EW components recorded at Port-island Kobe (PKB-NS, PKB-EW, Ground Type III).

The test cases are summarized in Table 5. The proposed curve approximate hysteresis model and

parameters obtain by quasi-static tests were used in the numerical nonlinear time history analysis for each case. In the ensuing section comparison between the pseudo-dynamic tests and numerical simulation analysis are discussed in terms of hysteresis loop shapes, displacement time histories, maximum displacements, residual displacements and energy dissipation.

Table 5. Tests and simulation cases

Specimen Type	S	Excitation Accelerograms					
		JMA (Ground Type I)		JRT (Ground Type II)		PKB (Ground Type III)	
		NS	EW	NS	EW	NS	EW
D450	4	- -	- -	No.1	No.2	- -	- -
D450	6	- -	- -	- -	No.3	- -	- -
D225	4	No.4	No.5	No.6	No.7	No.8	No.9
D150	4	- -	- -	No.10	No.11	- -	- -

4.1 Hysteresis loops and response displacement time histories

Figure 14 shows the hysteresis loops and displacement time histories for all cases. Results of pseudo-dynamic tests and simulations are plotted with solid and broken lines, respectively. In all cases the results of pseudo-dynamic test are shown to be successfully simulated using the proposed curve approximated model with a good accuracy.

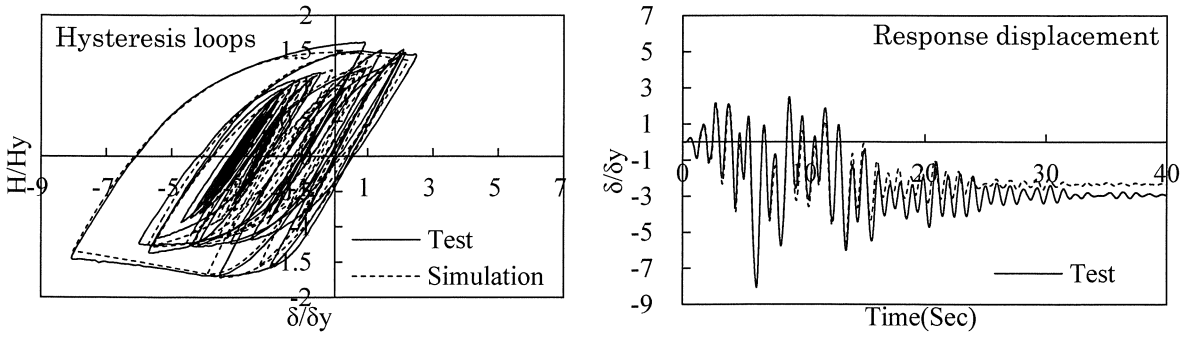

(a) No.1 (D450, S=4, JRT-NS)

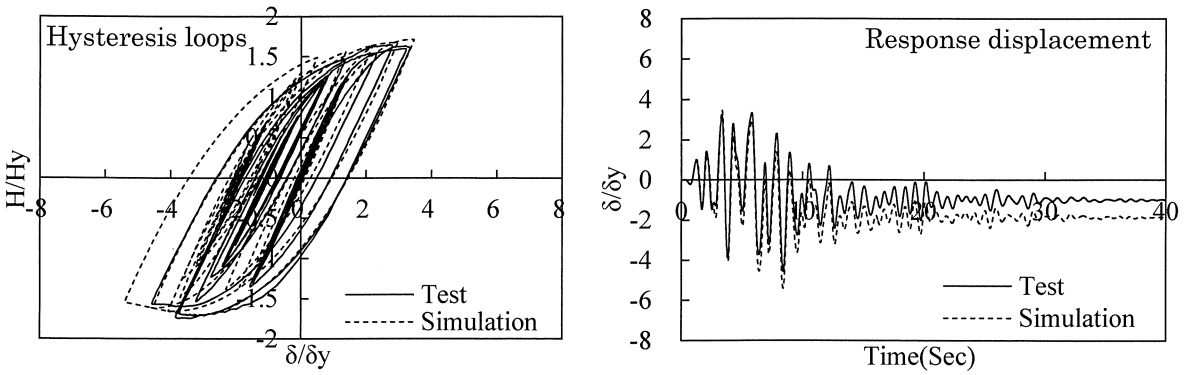

(b) No.2 (D450, S=4, JRT-EW)

Figure 14. Hysteresis loops and response displacement time histories

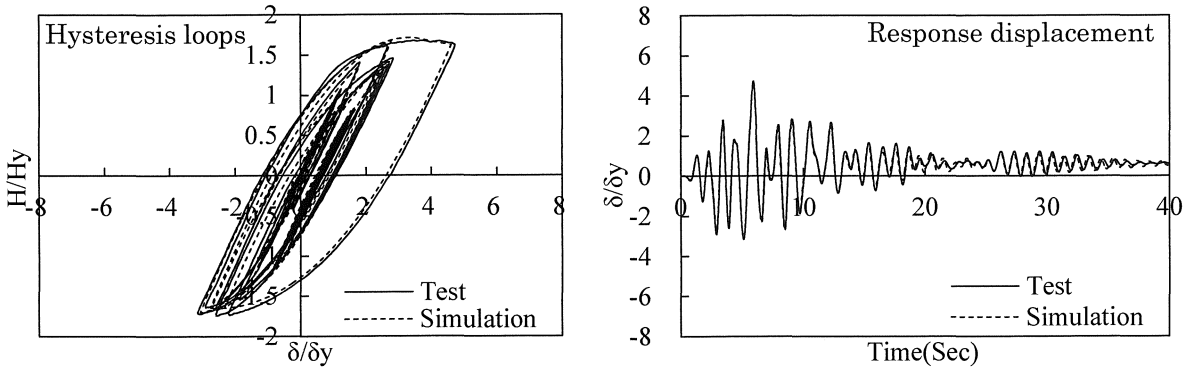

(c) No.3 (D450, S=6, JRT-EW)

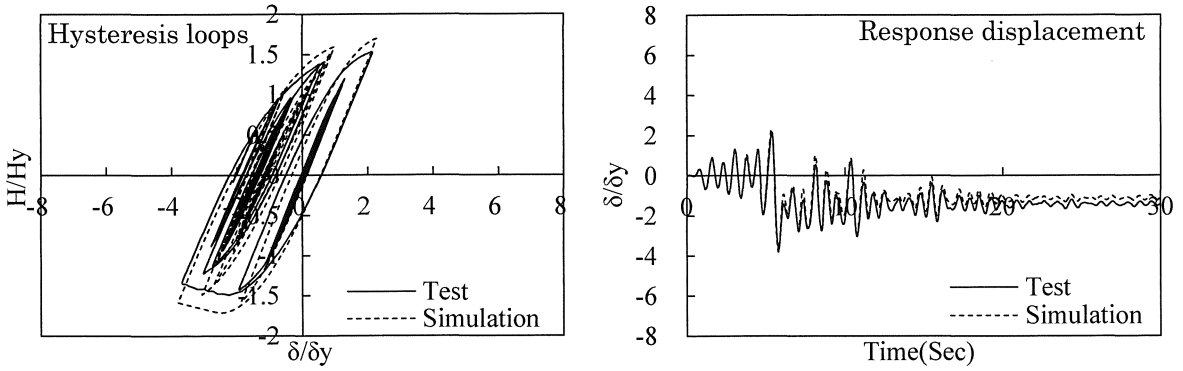

(d) No.4 (D225, S=4, JMA-NS)

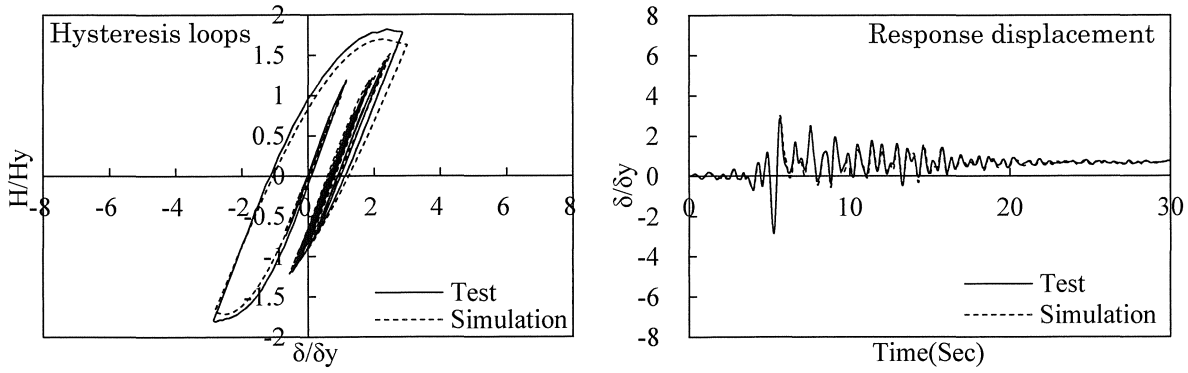

(e) No.5 (D225, S=4, JMA-EW)

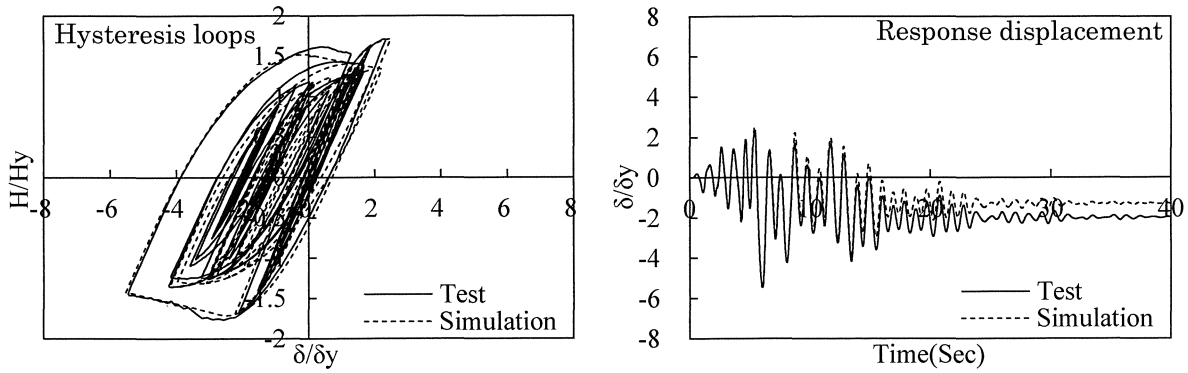

(f) No.6 (D225, S=4, JRT-NS)

Figure 14. Hysteresis loops and response displacement time histories (Continued)

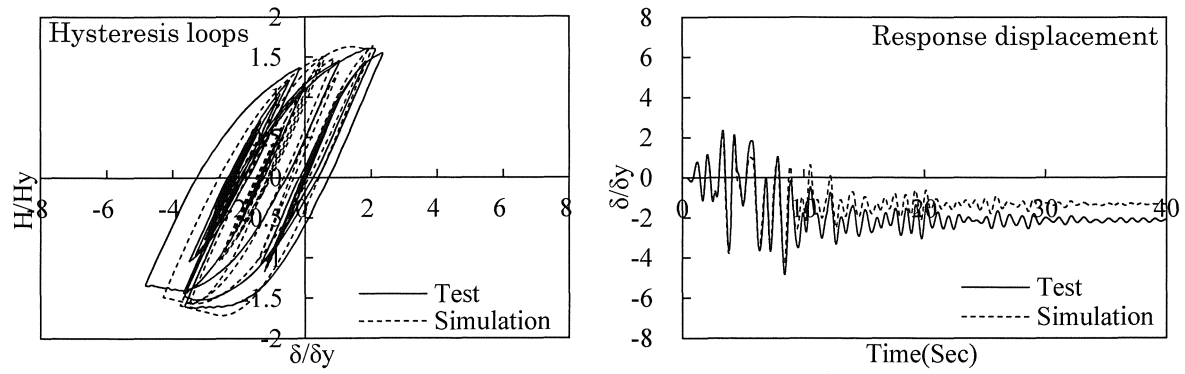

(g) No.7 (D225, S=4, JRT-EW)

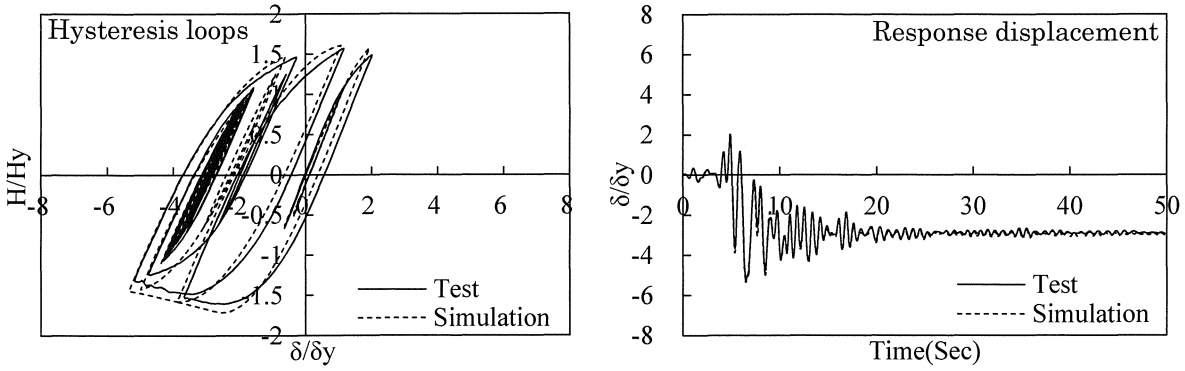

(h) No.8 (D225, S=4, PKB-NS)

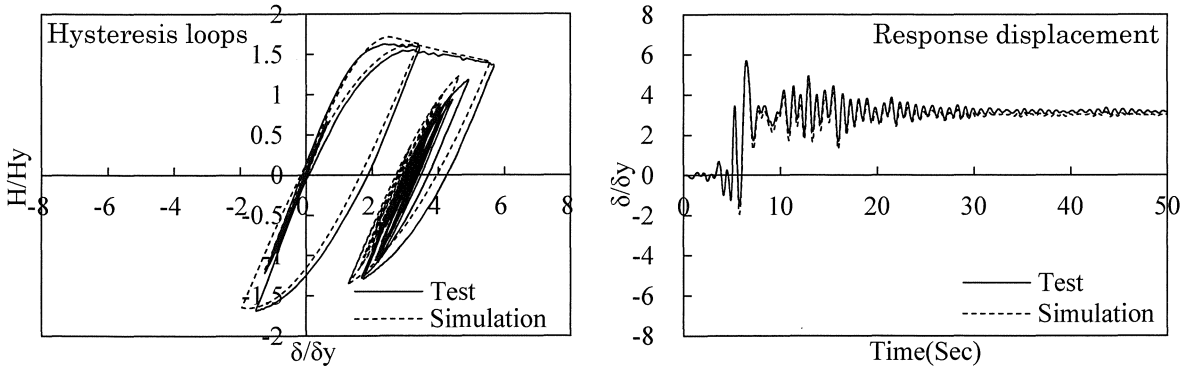

(i) No.9 (D225, S=4, PKB-EW)

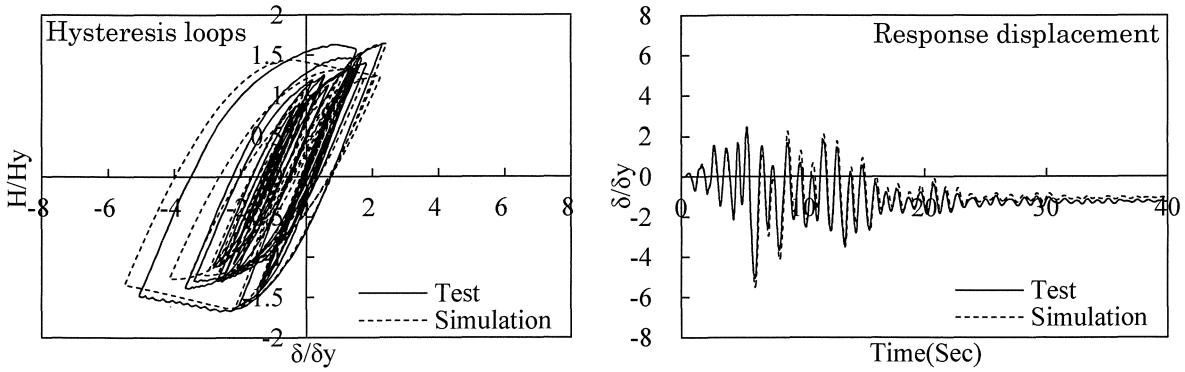

(j) No.10 (D150, S=4, JRT-NS)

Figure 14. Hysteresis loops and response displacement time histories (Continued)

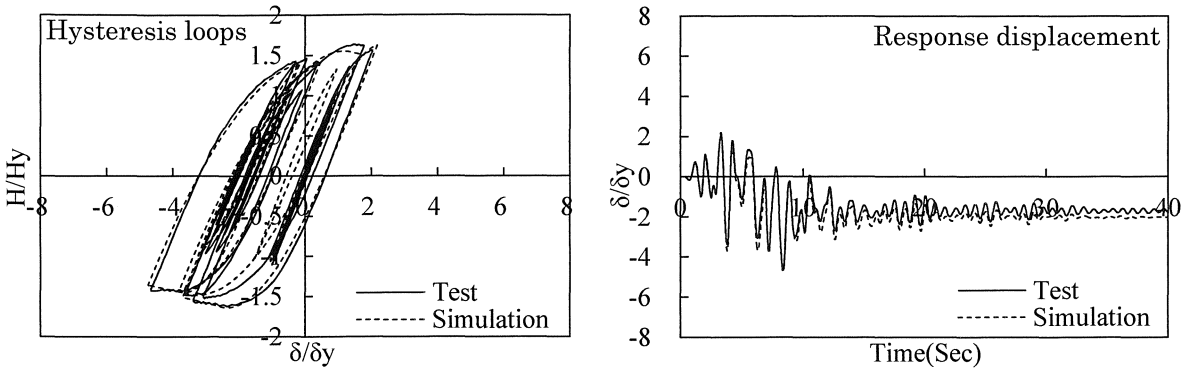

(k) No.11 (D150, S=4, JRT-EW)

Figure 14. Hysteresis loops and response displacement time histories (Continued)

4.2 Comparison of maximum displacement

The maximum displacement (δ_{max}) may be one of the most important indices in the performance-based seismic design. Figure 15 shows comparison of maximum response displacements in the test and simulation results. The maximum displacements computed by simulations are almost the same as that given by the pseudo-dynamic tests. The average error of the maximum response displacement in simulations compared with the pseudo-dynamic test result as small as 5%, and the difference is less than $1\delta_y$.

4.3 Comparison of residual displacement

The residual displacement (δ_r) is a main measure of repairability of highway after its damage due to major earthquake. Figure 16 shows the comparison of residual displacement obtained by tests and simulations. Accuracy of simulations in predicting the residual displacements is found to be acceptably good, as the relative error of the simulation as 22% compared with the test result, while the maximum difference corresponds to 0.35 δ_y.

4.4 Comparison of hysteresis energy dissipation

Generally, hysteresis energy dissipation due to tri-linear type nonlinear hysteresis models could be 15%~50% underestimated [9], that of bi-linear type model is even more. This may cause large error in damage evaluation in term of damage accumulation [10]. Accurate prediction of energy dissipation was an intractable issue to date.

Comparison of dissipated energy by the bridge pier obtained by tests and simulations is shown in Fig.17. The average error of the simulation in the hysteresis energy dissipation is as small as 4%. The energy dissipation or damage cumulative can be easily accessed by proposed model in high accuracy.

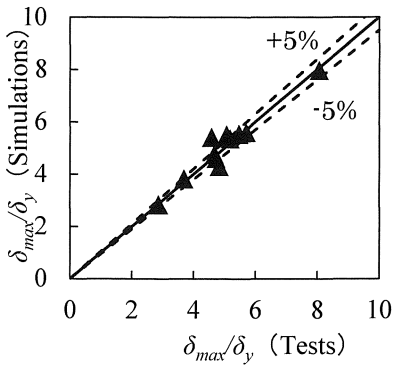

Figure 15. Comparison in δ_{max}

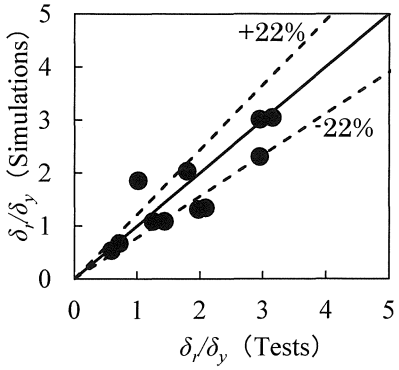

Figure 16. Comparison in δ_r

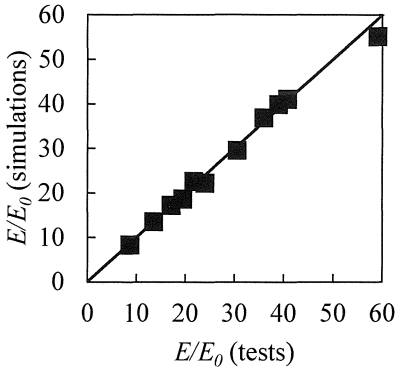

Figure 17. Comparison in E/E_0

5. CONCLUSIONS

In this paper, a curve approximated hysteresis model is proposed, based on the nonlinear hysteresis behavior of steel pier columns under particular emphasis on the unloading-reloading behavior, strength and stiffness degradation due to cumulative deterioration displacement (CDD) and associated increase of peak load point distance. Accuracy of the seismic response simulation using the proposed curve approximated hysteresis model is investigated by pseudo-dynamic tests. The fundamental concept of the curve approximated model may be as follows:

(1) The first peak load point of a steel pier is assumed to be constant and the hysteresis load-displacement response is represented by basic curves until the onset of deterioration.
(2) The unloading-reloading hardening character is taken into account by applying sub curves to connect hysteresis unloading points.
(3) The strength and stiffness degradations are expressed as functions of cumulative deterioration displacement, which is the cumulative displacement path length in the deterioration range.
(4) The distance between the two peak loading points and its increase due to cumulative deterioration is also approximated as a function of cumulative deterioration.

Parameters (δ_{m0}, H_{m0}), (δ_l, H_l), κ and γ to define the curve approximated model can be determined from quasi-static loading tests, static numerical analysis or empirical equations.

By comparing the results of eleven cases of pseudo-dynamic tests and corresponding nonlinear time history analysis using the proposed curve approximated hysteresis model, the differences of in maximum response displacement, residual displacement and energy absorption between the tests and the simulation are found to be as small as 5%, 22% and 4%, respectively.

REFERENCES

1. Usami,T., Imai,Y, Aoki,T. and Itoh Y.(1991). "An Experimental study on the Strength and Ductility of

Steel Compression Member under Cyclic Loading" Journal of Structural Engineering, JSCE, 37(A), 93-106 (in Japanese).

2. Usami,T., Mizutani,S., Aoki,T., Itou Y. and Yasunami, H.(1992). "An Experimental study on the Elasto-Plastic Cyclic Behavior of Stiffened Box Members" " Journal of Structural Engineering, JSCE, 38(A), 105-117 (in Japanese).
3. Usami,T., Banno,S., Zetsu,H. and Aoki,T. (1993). "An experimental study on the Elasto-Plastic Behavior of Compression Members under Cyclic Loading –Effect of Loading Program" Journal of Structural Engineering, JSCE, 39(A), 235-247 (in Japanese).
4. Suzuki,M., Usami,T. and Takemoto,K. (1995). "An Experimental study on Static and Quasi-Static Behavior of Steel Bridge Pier Models" Structure Eng./Earthquake Eng., JSCE, No.505(I-103), 99-108 (in Japanese).
5. Aoki,T., Ohnishi,A. and Suzuki,M. (2007). "Experimental study on the Seismic Resistance Performance of Rectangular Cross Section Steel Bridge Piers subject to Bi-Directional Horizontal Loads" Journal of Structural Engineering, JSCE, Vol.63(No.4), 716-726 (in Japanese).
6. Iemura,H. (1985). "Development and Future Prospect of Hybrid Experiments" Structure Eng./Earthquake Eng., JSCE, 356(I-3), 1-10 (in Japanese).
7. Saizuka,K., Itoh, Y., Kiso,E. and Usami,T. (1995). "A Consideration on Procedures of Hybrid Earthquake Responses Test taking account of the Scale Factor" Structure Eng. / Earthquake Eng., JSCE, No.505(I-30), 179-190 (in Japanese).
8. Usami,T., Saizuka,K., Kiso,E. and Itoh, Y. (1995). "Pseudo-Dynamic Tests of Steel Bridge Pier Model under Severe Earthquake" Structure Eng./Earthquake Eng., JSCE, No.519(I-32), 101-113 (in Japanese).
9. Suzuki,M., Usami,T., Terada M., Itoh, T. and Saizuka,K. (1996). "Hysteresis Models for Steel Bridge Piers and their Application to Elasto-Plastic Seismic Response Analysis" Structure Eng. / Earthquake Eng., JSCE, No.549(I-37), 191-204 (in Japanese).
10. Kindaichi T., Usami T., Satish K. (1998). "A hysteresis model based on Damage Index for steel bridge piers" Journal of Structural Engineering, JSCE, Vol.53(A), 667-678 (in Japanese).
11. Aoki,T., Suzuki,M. and Tanaka,T. (1998) "Multi-curve model for steel pier hysteretic curve" Proceedings of the Second Symposium on Nonlinear Numerical Analysis and its Application to Seismic Design of Steel Structures, Vol.2, 271-274 (in Japanese).
12. Usami,T. and Japan Society of Steel Construction (2006) "Seismic Resistance and Seismic control Design Guideline of Steel Bridge" Gijyututou Press, 128-129.
13. Vamvatsikos D. and Cornell C.A. (2002), "Incremental dynamic analysis" Earthquake Engineering and Structural Dynamics, Vol.31, 491-514.
14. Han S.W. and Chopra A.K. (2006), "Approximate incremental dynamic analysis using the modal pushover analysis procedure" Earthquake Engineering and Structural Dynamics,Vol.35, 1853-1873.
15. Design Specifications of Highway Bridges (Part V. Seismic Design), Japan Road Association, March 2002.
16. Iura,M., Kumagai,Y. and Komaki,O.(1997). "Ultimate Strength of Stiffened Cylindrical Shells

Subjected to Axial and Lateral Forces", Structure Eng./Earthquake Eng., JSCE, No.556, 107-118 (in Japanese).

17. Design Specifications of Highway Bridges (Part II. Steel Bridge), Japan Road Association, March 2002.
18. Ge H., Usami T., Gao S. (2000) "Numerical study on cyclic elastoplastic behavior of stiffened box-sectional steel bridge piers", Journal of Structural Engineering, JSCE, Vol.46(A), 109-118 (in Japanese).
19. Sibata, M. (2003) "Latest Seismic Resistance Analysis" Morikita Shuppan (in Japanese).
20. Dang J., Aoki T. (2012) "Bidirectional loading hybrid tests of square cross-sections of steel bridge piers", Earthquake Engineering and Structural Dynamics, Published online in Wiley Online Library.